Mechanism of GaN quantum dots capped with AlN: An AFM, electron microscopy, and x-ray anomalous diffraction study

J. Coraux,[1] B. Amstatt,[1] J. A. Budagoski,[1,*] E. Bellet-Amalric,[1] Jean-Luc Rouvière,[1] V. Favre-Nicolin,[1] M. G. Proietti,[2] H. Renevier,[1] and B. Daudin[1]

[1]*Department of Fundamental Research on Condensed Matter, CEA/Grenoble, 17 rue des Martyrs, 38054-Grenoble cedex 9, France*

[2]*Departamento Fisica de la Materia Condensada–ICMA - Centro Politécnico Superior, Universidad de Zaragoza, C. Maria de Luna 3, 50015 Zaragoza, Spain*

(Received 29 May 2006; revised manuscript received 28 August 2006; published 2 November 2006)

Capping of GaN quantum dots with AlN has been studied at the monolayer scale by combining atomic force microscopy, high resolution electron microscopy, and grazing incidence x-ray anomalous diffraction. Consistent with the results provided by these three techniques, it has been demonstrated that, following a wetting of the dots by an AlN layer up to 4 ML coverage, subsequent capping is dominated by a preferential AlN growth in between the dots, eventually resulting in a complete smoothing of AlN. Interdiffusion has been shown to be negligible during this process, which makes the GaN/AlN system unique among semiconductors.

DOI: 10.1103/PhysRevB.74.195302 PACS number(s): 61.46.−w, 61.10.Nz, 61.10.Ht, 68.65.Hb

I. INTRODUCTION

Quantum dots (QDs) of semiconductors have been a subject of constant interest for several decades due to their specific physical properties. In particular, the small size of QDs makes them relatively insensitive to the structural defects of the surrounding matrix, leading to remarkable optical properties. Noticeably, carrier confinement in QDs often results in an absence of photoluminescence quenching at room temperature (or in a reduced one), which makes them promising candidates for the active region of highly efficient light emitting diodes (LEDs).

The practical realization of devices implies capping of the QDs by barrier material. Actually, this simple operation may drastically modify the morphology and/or the optical properties of the QDs. Depending on growth conditions, capping of QDs may result in either an increase or a decrease of their size, which results from specific chemical reactions at the interface such as, for instance, dot/barrier interdiffusion in the most studied case of InAs QDs capped by GaAs or AlAs (Refs. 1–6) or enhanced migration in the case of Si/Ge system.[7–10]

As far as GaN/AlN system is concerned, which is the most recent member of the family of self-assembled QDs system,[11] it has been demonstrated that capping of GaN QDs by AlN results in a size decrease due to atomic vertical exchange between Ga and Al, driven by the greater thermodynamic stability of AlN compared to GaN.[12] It has to be noted that this process is limited to two monolayers (ML) and is not thermally activated. Actually, the AlN/GaN system presents the remarkable characteristics of being almost insensitive to interdiffusion,[13] which makes it of particular interest for studying capping-induced strain in QDs.

Changes in the QD strain state are expected for every system, due to the lattice mismatch between QD and capping barrier, possibly complicated by interdiffusion (and therefore changes in chemical composition) in both QD and barrier. In the particular case of GaN QDs, the optical properties of which are dominated to a large extent by the presence of a piezoelectric field,[14] capping-induced strain changes are of drastic importance. It has been previously demonstrated that vertical arrangement of dots may be observed, depending on the thickness of AlN spacers between successive planes of GaN QDs.[15] As recently put in evidence by quantitative analysis of transmission electron microscopy pictures, the driving force of this mechanism is the strain exerted by GaN QDs on the surrounding AlN matrix.[13] Raman[16] and x-ray diffraction experiments[17–19] have shown that the elastic interaction between GaN dots and the surrounding AlN matrix is complex and depends on the number of stacked QDs planes.

As a whole, in-depth understanding of QDs capping is necessary to predict their optical properties or to possibly adjust them: along these views, it is the aim of this paper to analyze in details the case of GaN QDs capped with AlN. In a recent paper, we have paid particular attention to the strain state of capped GaN QDs and also presented preliminary results indicating that the AlN capping of the dots followed a two-step mechanism.[19] Following this previous work, it is our goal to examine here in details the AlN capping mechanism at the monolayer scale. For this purpose, we have used a combination of complementary experimental techniques, namely atomic force microscopy (AFM), high resolution electron microscopy (HREM), and x-ray anomalous diffraction. We will show that a two-step capping process takes place. The first step consists of uniform wetting of GaN QDs with AlN whereas, during the second one, preferential growth of AlN in between the dots leads to a rapid smoothing of the capping layer, which was typically achieved in the present case for the deposition of 14 ML of AlN.

II. EXPERIMENTS

The samples used in this work were grown by molecular beam epitaxy (MBE). The substrate was commercial (0001)SiC which was polished by NovaSiC Company. Following standard chemical cleaning, it was introduced in a MBE machine equipped with Ga and Al effusion cells and with an rf-plasma cell for active *N* production.

After deposition of a thin AlN buffer layer (about 5 nm), GaN QDs were grown using the modified Stranski-

 ©2006 The American Physical Society

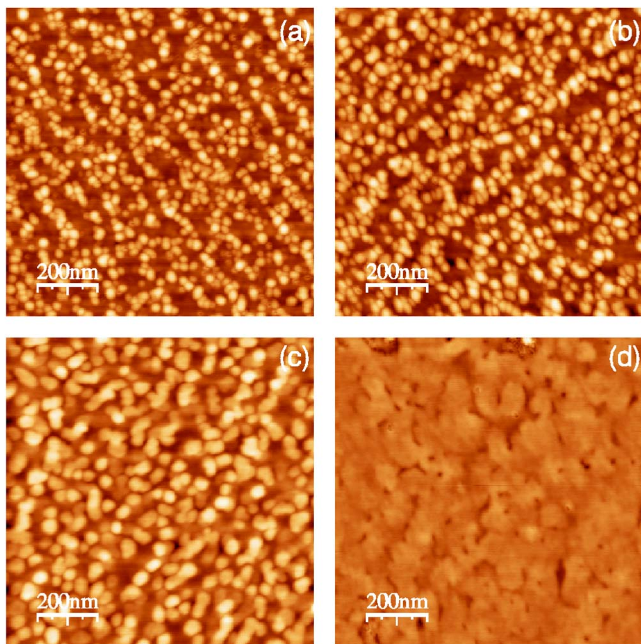

FIG. 1. (Color online) AFM images of GaN dots progressively capped by AlN. (a) Uncapped, (b) 4 MLs AlN, (c) 11 MLs AlN, and (d) 18 MLs AlN.

Krastanow (SK) growth mode[20] by depositing at 740 °C the equivalent of 4 GaN ML in Ga-rich conditions. Following desorption of Ga film under vacuum, GaN QDs were formed and let evolve during 1 min under vacuum. Next, the dots were capped with AlN of various thicknesses, namely 2, 4, 8, 11, 14, 18, and 20 ML.

An additional sample was grown, which was specially designed to fit the requirements of electron microscopy. It was grown in the same conditions as described above and consisted of several units of three stacked planes of GaN QDs embedded in AlN. The last plane of dots of each three-plane unit was covered with 4, 8, 11, and 14 ML of AlN, respectively. Next, a 2 ML thick GaN layer, below the critical thickness for the three-dimensional (3D) island formation, was deposited before further AlN growth, with the purpose of making the morphology of the thin AlN capping layer visible. After deposition of this GaN marker layer, AlN growth was resumed until the complete smoothing of the surface, before the growth of the next three-plane unit.

A. Atomic force microscopy

Atomic force microscopy experiments in tapping mode were performed to study the variation of surface morphology as a function of the AlN capping thickness. Samples were found to be homogeneous. Statistics were performed by analyzing an average of 100 dots per sample. Error bars in Figs. 2 and 3 correspond to the standard deviation of the Gaussian distribution of the experimental data.

As shown in Fig. 1, a progressive change in the surface morphology is observed, namely a smoothing and a diameter increase of islands (i.e., QDs *plus* AlN capping layer) present on the surface, which is associated with progressive AlN capping. The statistical analysis of the capped islands is shown in Figs. 2 and 3. In Fig. 2, their height and diameter are plotted as a function of AlN capping. No change is observed up to an AlN coverage of 4 ML. Next, further AlN capping is associated with height decrease and diameter increase, as an evidence of progressive smoothing of the surface. The evolution of the height/diameter aspect ratio is shown in Fig. 3: it is about 0.08 for uncovered dots and up to 4 ML AlN coverage, then it progressively decreases to about 0.02 for an AlN coverage of 20 ML, showing a dramatic flattening of the islands.

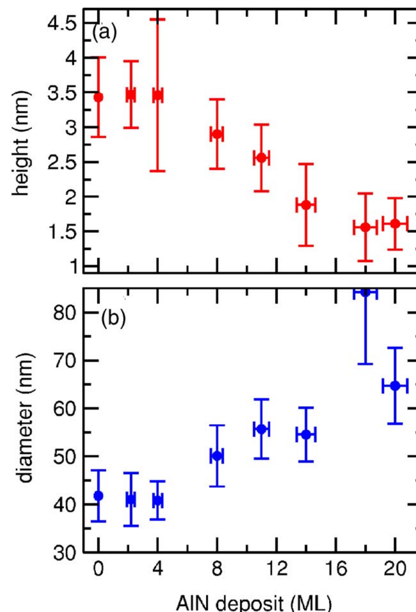

FIG. 2. (Color online) (a) height and (b) diameter of the uncapped/capped GaN islands as a function of AlN capping thickness.

B. High resolution electronic microscopy

Further understanding of AlN capping process at the monolayer scale was obtained by performing transmission electron microscopy (TEM) experiments using the dedicated sample described in Sec. II, with GaN marker layers visual-

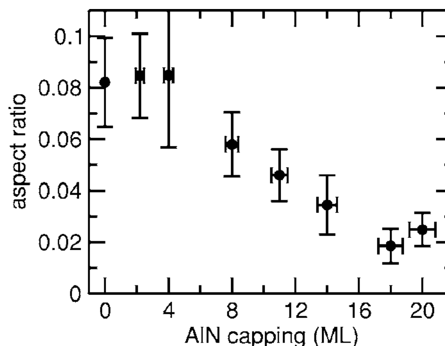

FIG. 3. rms roughness of the surface as a function of AlN capping thickness. Note the progressive smoothing above 4 ML AlN coverage.

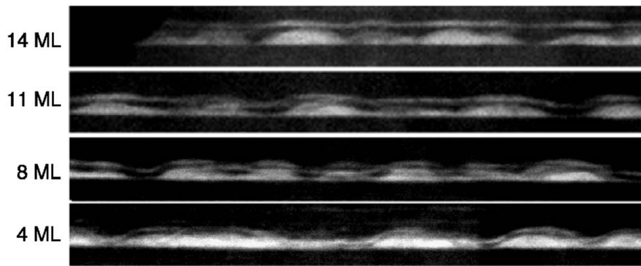

FIG. 4. *Z*-contrast STEM images showing the capping of GaN dots with 4, 8, 11, and of 14 MLs AlN. The white line above the GaN dots and AlN thin layer is the GaN marker which allows one to observe the morphology variation of AlN as a function of coverage. Note that the distance between the bottom of dots and the marker at the apex of dots does not depend on AlN coverage in the studied range.

izing the morphology of the successive AlN capping layers. *Z*-contrast images were realized on a FEI Titan microscope working at 300 kV. A Fishione HAADF detector was used. Low magnification images were first realized for a general view of the sample. The main features are observed in classical *Z*-contrast images. The results are summarized in Fig. 4, which shows the last GaN dot plane of the four three-unit stacks. The AlN capping layers have nominal thicknesses of 4, 8, 11, and 14 ML, respectively. The GaN marker layer can be clearly seen on top of the GaN dots. Superposition of several dots in the projected TEM image was avoided by selecting a relatively thin observed area. However, such a superposition can be detected in the left part of the 4 ML image of Fig. 4. It is also responsible of the peculiar contrast in the 8 ML image.

One can see in Fig. 4 that the 4 ML thick AlN layer wets the GaN dots whereas in the case of the 14 ML thick AlN capping layer, the bottom part of the GaN marker layer is nearly flat. Just above the GaN dots, the upper part of the GaN marker exhibits a slight roughness, precursory of the two-dimensional (2D)/3D transition. This is consistent with the fact that the thickness of the GaN marker is just below the critical thickness for 2D/3D transition.[21] However, as a key feature, it has to be noted that the distance between the base of the dots and the bottom part of the marker layer at the apex of the bigger GaN dots does not change with AlN coverage. This puts in evidence that, after wetting of the dots with a 4 ML thick AlN layer, subsequent AlN growth preferentially occurs in between the dots. Based on the AFM data, it is worth noting that 14 ML AlN coverage roughly corresponds to the quantity of AlN necessary to fill the space between dots, which presumably depends on the actual density and size of GaN dots.

More insight is provided by high resolution scanning transmission electron microscopy (HR-STEM). Figure 5 shows HR-STEM images taken along a $\langle 2\bar{1}\bar{1}0\rangle$ direction. In addition to the true projection of the atomic columns given by HR-TEM, HR-STEM images provides a chemical information as the signal detected by the annular detector is approximately proportional to Z^{α}, where Z is the average atomic number of the atomic column and α is a factor equal to about 2.[22] Actually, the average intensity is also sensitive,

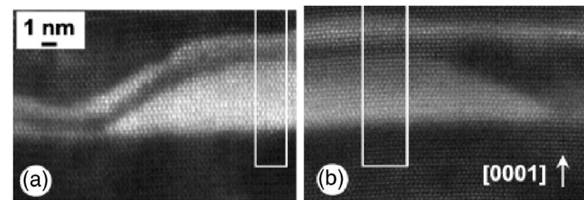

FIG. 5. HR-STEM images taken along a $\langle 2,-1,-1,0\rangle$ direction. The white dots correspond to the projection of two adjacent atomic columns containing respectively *N* and Ga/Al atoms. The vertical white box indicates the integration area selected for extracting the projected profile in Fig. 6(a) GaN dots covered with a 4 ML AlN layer and a 4 ML GaN marker layer. (b) GaN dots covered with a 14 ML AlN layer and a nominal 4 ML GaN marker layer. The slight bending of the (0002) planes on the image is due to a small drift of the sample during the acquisition of the scanned image.

but to a minor extent, to slight crystal disorientation, surface roughness and surface defect layers created during the TEM specimen preparation, which prevents from extracting accurate chemical information from the intensity. As a matter of fact, the intensity variations that occur in the AlN layers below the GaN dots, as shown in Fig. 5, are likely due to these effects and not to Ga/Al intermixing. It should also be noted that the HR-STEM images only give a projection of the 3D structure. Consequently, it is not sure that the whole quantum dot is observed and it is furthermore likely that AlN-related information is systematically present in the image. All these features strongly limit the accuracy of the quantitative analysis of HR-STEM images. This can be improved by extracting intensity profiles, as shown in Fig. 6. Noticeably, the tiny oscillations are due to atomic (0002) planes, which correspond to 1 ML of deposited material, the average intensity being, as recalled before, mainly a function of chemicals. The typical uncertainty in such profiles is slightly lower than 1 ML.

The following trends can be observed in Fig. 6:

(i) The GaN wetting layer in between the GaN dots spans over approximately 3–4 ML, and the two central ML exhibit

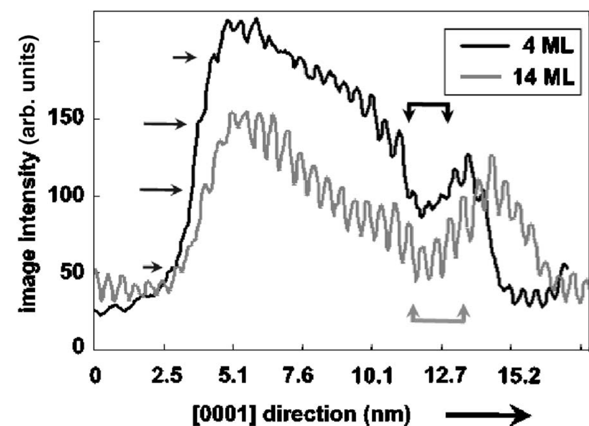

FIG. 6. Average intensity profile of HR-STEM images of Fig. 5. The atomic (0002) planes, corresponding to 1 ML, are seen. The horizontal arrows show the transition planes between the AlN matrix and the GaN dot. The vertical arrows point out the AlN planes of the AlN capping layer which is followed by the GaN marker layer.

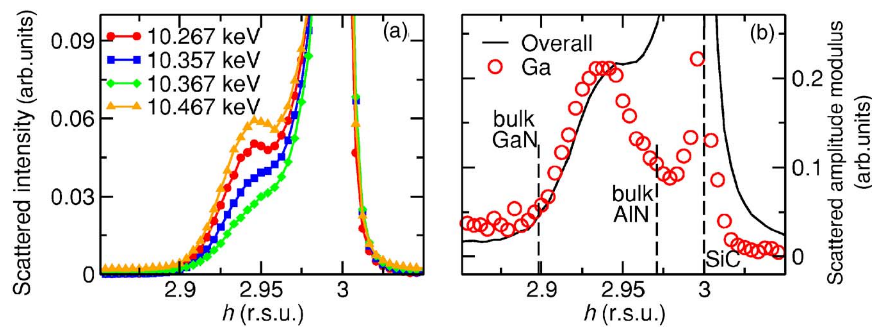

FIG. 7. (Color online) (a) Diffracted intensity measured at four energies across the Ga K edge (10.367 keV), along the [10-10] reciprocal space direction, labeled in reciprocal space units (r.s.u.) by h. $h=3$ is the position of the SiC substrate, used as a scale reference. (b) Extracted modulus of the Ga regions scattered amplitude, as deduced by MAD, compared to the square root of the overall scattered intensity measured at 10.267 keV. Grazing incidence angle, $\alpha_i=0.3°$.

a richer Ga content. This result is consistent with HR-TEM studies which demonstrated that the wetting layer extends on four planes, with a graded Ga composition.[23]

(ii) The transition between the AlN matrix and the bottom of the GaN dot also extends on 3–4 ML. This can be checked on the profiles in Fig. 6, where the four atomic planes are shown by horizontal arrows. It should be noticed that the lower and upper horizontal arrows in Fig. 6 are nearly at the level of the AlN matrix and the GaN dot, respectively, indicating that their chemical compositions are very close to that of the pure binary material.

(iii) In the 4 ML case, the thickness of the AlN capping layer is almost constant, independent of position with respect to the dot. This can be checked quantitatively. At the apex of the GaN dots, on their lateral sides and above the GaN wetting layer, the measured AlN thickness extracted from the average intensity profile of HR-STEM images are 0.81 nm±0.1 nm, 0.89 nm±0.1 nm, and 0.7 nm±0.1 nm, respectively, which strongly suggests a uniform AlN wetting.

(iv) As observed in low magnification STEM images (Fig. 4), the quantity of AlN which is located at the apex of the dot does not change significantly for the four AlN coverages which were studied. About 3–4 ML of AlN can be detected at the apex of the dots.

In Fig. 6, a regular intensity decrease as a function of position is observed in the GaN dot area. As discussed above, this results from a projection effect related to the geometry of the GaN dot and to superposition of the surrounding AlN matrix. The discontinuity at the end of the sloppy part of the profile can be used to determine the beginning of the AlN capping layer. In the 4 ML profile, three AlN-rich planes can be unambiguously identified, followed by a GaN marker layer of about 4 ML, corresponding to the nominal amount deposited. From average intensity analysis, an AlN thickness of about 0.8 nm is found (vertical arrows in Fig. 6). In the 14 ML profile, only two AlN-rich planes can be detected, but the following GaN marker layer extends on 7 ML and the AlN thickness extracted from the average intensity measurement (vertical arrows in Fig. 6), is about 0.9 nm. This thickness is similar to the value of the 4 ML case. The value of 7 ML for the GaN marker layer at the apex of the dot presumably originates from a roughening precursory to the formation of GaN dot. As a matter of fact, it can be visually checked on Fig. 5 that the GaN marker layer is thicker at the apex of the GaN dot. Furthermore, as can be checked in Fig. 4 by comparison with the other cases, the GaN marker layer thickness in the 14 ML stack is thicker than the nominal value of 4 ML and is closer to 5 ML.

In summary, HR-STEM images confirm the trends of the low magnification images and allow one to quantify the thickness of the different parts of the structure. Note that at this stage uncertainties lower than 1 ML regarding thickness are still difficult to achieve.

C. X-ray anomalous diffraction experiments

Complementary information regarding the capping process was achieved by means of x-ray anomalous diffraction, in grazing incidence to enhance the contribution of the dots and AlN capping with respect to that of the substrate. This study was performed on a set of 6 of the samples described above and previously studied by AFM, namely those with an AlN deposit of 0, 2, 4, 8, 11, and 18 ML, respectively. The average height and diameter, as determined by AFM were found to be 3.5 nm and 40 nm respectively. The x-ray measurements were performed at the French Collaborative Research Group beamline BM2 at the European Synchrotron Radiation Facility (ESRF), using the 8-circles diffractometer equipment.[24]

Due to the small (2.5%) lattice mismatch between GaN and AlN and the small finite size of the dots, the diffraction peaks do noticeably overlap in reciprocal space. Moreover, a simple deconvolution of the GaN and AlN contributions is impossible because the measured scattered intensity provides the overall squared scattered amplitude. However, by varying the scattering power of one element, for instance Ga, it is possible to localize specifically GaN regions in reciprocal space. This is the purpose of anomalous diffraction measurements, which consists in recording the scattered intensity as a function of the energy across the absorption edge of an element, namely Ga in the present case.

First, multiwavelength anomalous diffraction (MAD) was performed in grazing incidence, with roughly 10 energies across the Ga K edge (10.367 keV), to localize Ga along the $[10\bar{1}0]$ reciprocal space direction, which is sensitive to the in-plane strain and structure. Figure 7(a) shows scattered in-

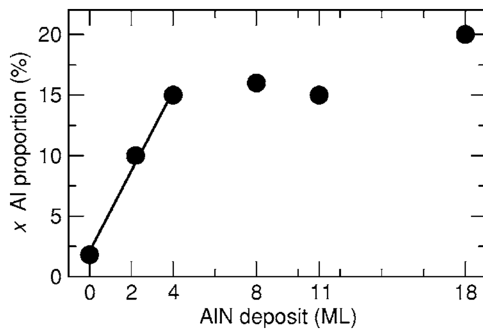

FIG. 8. Al proportion x of the isostrain region, as a function of the AlN deposit on top of the QDs plane.

tensities measured along the $[10\bar{1}0]$ direction at four, out of the ~10, energies across the Ga K edge. The resulting scattered amplitude modulus from Ga regions, extracted according to the MAD principles,[18,19,25] is shown in Fig. 7(b), together with the square root of the overall scattered intensity at 10.267 keV for comparison. The position of the Ga signal maximum along $[10\bar{1}0]$ is directly related to the average in-plane strain state in the QDs.

Further anomalous diffraction experiments were performed, selecting specifically the QDs by measuring the scattered intensity at the maximum of the Ga partial structure factor determined by MAD. The incident angle was set to $\alpha_i=0.3°$, which is slightly above the critical angle for which total reflection regime takes place (~0.20° for AlN).

The energy was varied with a 2 eV energy step from 10.2 keV to 10.8 keV, including the extended diffraction anomalous fine structure oscillations region above the Ga K edge. The smooth variations (disregarding oscillations) of the diffracted intensity, more precisely the cusp at the edge, were fitted using a least-squares algorithm to assess the structural, crystallographic parameters related to the isostrain region selected by diffraction.[19,26,27]

Figure 8 shows the variation of the x Al/Ga proportion of the isostrain volume selected by diffraction at the maximum of the Ga partial structure factor, as a function of the AlN deposit on top of the QDs planes (see Sec. VI in Ref. 19). Up to 4–5 ML, the Al proportion, which is near to zero for free standing QDs (0.19±0.01%) increases linearly, and stabilizes above 4–5 ML, the contribution at 10 ML being almost the same as for 5 ML. Provided that AlN on top of the QDs is pseudomorphic to GaN for low coverages,[18] and as no appreciable intermixing occurs inside the GaN QDs,[19,28] the variation of the Al proportion x in the isostrain region up to 4–5 ML indicates a uniform increase of the amount of AlN on top of the GaN QDs. This could result from a uniform growth of AlN on the whole surface, i.e., the QDs and the thin pseudomorphic wetting layer,[29] as also indicated by the AFM and HRTEM analysis. The further evolution of the Al concentration above 4–5 ML points out a change in the AlN growth process, which leads to AlN with an in-plane strain state different from that in the QDs. These results are consistent with AFM and HRTEM data described above. In particular, it confirms that AlN monotonously grows on GaN up to 4 ML. Above this value, the regime change put in evidence by x-ray measurements is assigned to the selective AlN growth in between of the QDs, with a different strain with respect to the top QDs.

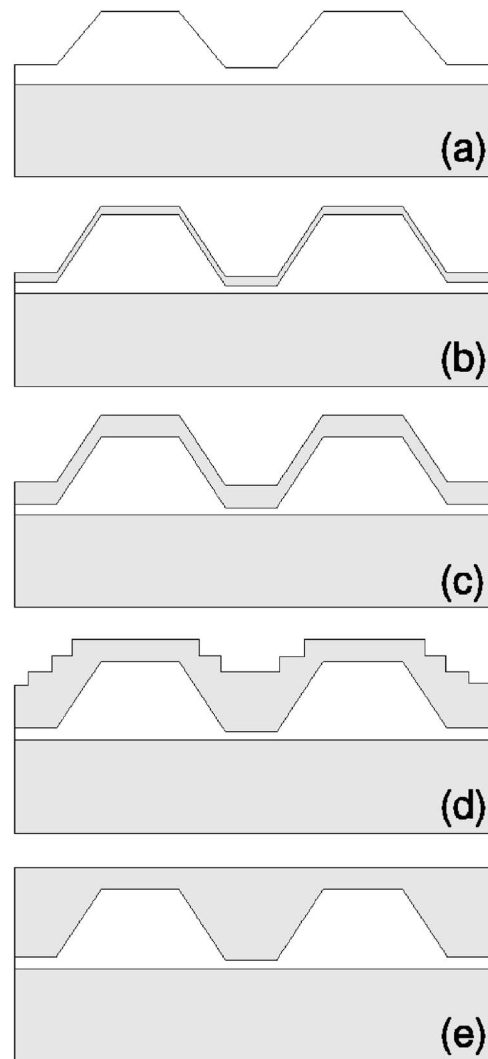

FIG. 9. Schematics of GaN QDs capping with AlN. (a) GaN dots are grown on AlN surface (b) vertical exchange between Ga and Al results in a decrease of the dot size by 1 ML. (c) Wetting of dots by AlN is observed up to a coverage of 4 MLs. (d) Next, preferential AlN growth is observed in between dots (e) smoothing of AlN is eventually observed.

III. DISCUSSION AND CONCLUSION

In this paper we use a multitechnique approach to demonstrate that the capping mechanism of GaN QDs by AlN takes place in two steps: wetting of QDs by a uniform AlN layer followed by intervalley filling. A layer of QDs deposited on AlN [Fig. 9(a)], is exposed to Al and N fluxes and wetting of the dots with a thin layer of AlN is observed [Fig. 9(b)]. This wetting is driven by the vertical exchange between Al and Ga atoms, which leads to the formation of more thermodynamically stable Al-N bonds and also to the size reduction of GaN QDs, as demonstrated in a previous work.[28] In the following step [Fig. 9(c)], up to a coverage of about 3–4 ML, AlN homogeneously covers the dots and the

space between them. AlN growth on top of the dots during this stage is unexpected as it implies an elastically unfavourable expansion of AlN lattice parameter. It may be, instead, of kinetical origin, due to the relatively low mobility of Al adatoms on the surface in the range of growth temperatures used. Above a coverage of 3–4 ML, the excess of accumulated elastic energy however leads to a drastic regime change which is more favourable from the elastic energy point of view: growth of AlN takes place in between of the QDs [Fig. 9(d)], preferentially filling the space in between of them. Eventually, further growth of AlN [Fig. 9(e)] leads to the recovery of a smooth surface.

A remarkable property of the GaN QDs is that they do not change in shape and that no significant AlN/GaN interdiffusion can be put in evidence during the capping process. This makes the case of AlN/GaN system drastically different from that of Si/Ge. For the latter, capping of Ge islands is associated with a progressive alloying and with a shape change. It has been recently argued that the Ge-Si intermixing, which is experimentally observed, is strain driven rather than thermally activated,[29] acting as driving force for the minimization of elastic energy of dots. As a further example of strain driven composition of the capping material, it is worth mentioning the case of InAs islands capped with InAlAs material which has been experimentally[30] and theoretically[31] studied in detail. In this case, an anisotropic strain-induced demixing of the capping material has been observed, eventually leading to a nontop-on-top vertical correlation of stacked nanostructures.

Another key parameter of capping process is the ability of the barrier material to wet the dots or not. Such ability is related, on one side, to the lattice parameter mismatch between islands and capping material which may either favor or not wetting. On the other side, the relative bond strength of dot and barrier material constitutes an additional parameter for wetting. Actually, it is found that despite the 2.5% lattice mismatch between AlN and GaN, AlN wets both GaN QDs and the GaN wetting layer in between of them. It is likely indeed, that the greater bond strength of AlN compared to GaN is responsible for this behavior, as it presumably prevents the surface migration of Al from the GaN QD to the GaN wetting layer at the base of them. Such a view is consistent with the vertical exchange between Ga and Al which has been observed when capping GaN quantum wells or QDs with AlN.[28] We believe that the ability of AlN to wet GaN is responsible for the first stage of homogeneous capping. Further deposition of AlN is governed by a trade-off between competing factors: deposition of AlN on dots results in dramatic straining of GaN QDs,[18] which partly compensates the expansion of AlN due to the lattice mismatch. Finally, our experimental results suggest that the AlN coverage of about 3–4 ML corresponds to a drastic change in the capping regime and to the onset of preferential growth of AlN in between the dots with respect to growth right over partially relaxed dots.

A further and interesting aspect of this work, on a methological point of view, is the combination of electron and atomic force microscopic techniques with a unique application of diffraction, namely DAFS, which allows one to confirm and quantify the AFM and HRTEM results on a statistically averaged scale.

ACKNOWLEDGMENTS

The authors (J.A.B. and M.G.P.) are thankful to the Ministry of Science and Technology of Spain (Grants MAT2003-00399 and MAT-2002-01221) for financial support. We also thank C. Priester and J. Villain for fruitful discussion and V. Salvador for the TEM sample preparation.

*On leave from the Institut de Ciència del Materials, Universitat de València, P.O. Box 22075, E-46071 València, Spain.

[1] F. Ferdos, S. Wang, Y. Wie, M. Sadhegi, Q. Zhao, and A. Larsson, J. Cryst. Growth **251**, 145 (2003).
[2] H. Heidemeyer, S. Kiravittaya, C. Muller, N. Y. Jin-Phillipp, and O. G. Schmidt, Appl. Phys. Lett. **80**, 1544 (2002).
[3] P. B. Joyce, T. J. Krzyzewski, G. R. Bell, and T. S. Jones, Appl. Phys. Lett. **79**, 3615 (2001).
[4] J. M. Garcia, G. Medeiros-Ribeiro, K. Schmidt, T. Ngo, J. L. Feng, A. Lorke, J. Kotthaus, and P. M. Petroff, Appl. Phys. Lett. **71**, 2014 (1997).
[5] J. M. Gérard, J. Y. Marzin, G. Zimmermann, A. Ponchet, O. Cabrol, D. Barrier, B. Jusserand, and B. Sermage, Solid-State Electron. **40**, 807 (1996).
[6] X. W. Lin, Z. Liliental-Weber, J. Washburn, E. R. Weber, A. Sasaki, A. Wakahara, and Y. Nabetani, J. Vac. Sci. Technol. B **12**, 2562 (1994).
[7] M. Kummer, B. Vogeli, and H. Von Kanel, Mater. Sci. Eng., B **69**, 247 (2000)
[8] P. Sutter and M. G. Lagally, Phys. Rev. Lett. **81**, 3471 (1998).
[9] Z. Zhong, J. Stangl, F. Schaffler, and G. Bauer, Appl. Phys. Lett. **83**, 3695 (2003).
[10] A. Hesse, J. Strangl, V. Holy, T. Roch, G. Bauer, O. G. Schmidt, U. Denker, and B. Struth, Phys. Rev. B **66**, 085321 (2002).
[11] B. Daudin, F. Widmann, G. Feuillet, Y. Samson, M. Arlery, and J. L. Rouvière, Phys. Rev. B **56**, R7069 (1997).
[12] N. Gogneau, D. Jalabert, E. Monroy, E. Sarigiannidou, J. L. Rouvière, T. Shibata, M. Tanaka, J. M. Gerard, and B. Daudin, J. Appl. Phys. **96**, 1104 (2004).
[13] E. Sarigiannidou, A. D. Andreev, E. Monroy, B. Daudin, and J. L. Rouvière, Appl. Phys. Lett. **87**, 203112 (2005).
[14] T. Gleim, L. Weinhardt, T. Schmidt, R. Fink, C. Heske, E. Umbach, L. Hansen, G. Landwehr, A. Waag, A. Fleszar, B. Richter, C. Ammon, M. Probst, and H. P. Steinruck, Phys. Rev. B **67**, 205315 (2003).
[15] F. Widmann, B. Daudin, G. Feuillet, Y. Samson, J. L. Rouvière, and N. Pelekanos, J. Appl. Phys. **83**, 7618 (1998).
[16] A. Cros, N. Garro, J. M. Llorens, A. Garcia-Cristobal, A. Cantarero, N. Gogneau, E. Monroy, and B. Daudin, Phys. Rev. B **74**, 075305 (2006).
[17] V. Chamard, T. H. Metzger, M. Sztucki, V. Holy, M. Tolan, E. Bellet-Amalric, C. Adelmann, B. Daudin, and H. Mariette, Eu-

rophys. Lett. **63**(2), 268 (2003)

[18] J. Coraux, H. Renevier, V. Favre-Nicolin, G. Renaud, and B. Daudin, Appl. Phys. Lett. **88**, 153125 (2006).

[19] J. Coraux, V. Favre-Nicolin, M. G. Proietti, H. Renevier, and B. Daudin, Phys. Rev. B **73**, 205343 (2006).

[20] N. Gogneau, D. Jalabert, E. Monroy, T. Shibata, M. Tanaka, and B. Daudin, J. Appl. Phys. **94**, 2254 (2003).

[21] C. Adelmann, B. Daudin, R. A. Oliver, G. A. D. Briggs, and R. E. Rudd, Phys. Rev. B **70**, 125427 (2004).

[22] S. J. Pennycook, Ultramicroscopy **30**, 58 (1989).

[23] M. Arlery, J.-L. Rouvière, F. Widmann, B. Daudin, G. Feuillet, and H. Mariette, Appl. Phys. Lett. **74**, 3287 (1999).

[24] H. Renevier, S. Grenier, S. Arnaud, J. F. Bérar, B. Caillot, J. L. Hodeau, A. Letoublon, M. G. Proietti, and B. Ravel, J. Synchrotron Radiat. **10**, 435 (2003).

[25] A. Létoublon, V. Favre-Nicolin, H. Renevier, M. G. Proietti, C. Monat, M. Gendry, O. Marty, and C. Priester, Phys. Rev. Lett. **92**, 186101 (2004).

[26] M. G. Proietti, H. Renevier, J.-L. Hodeau, J. García, J.-F. Bérar, and P. Wolfers, Phys. Rev. B **59**, 5479 (1999).

[27] H. H. Lee, M. S. Yi, H. W. Jang, Y. T. Moon, S.-J. Park, D. Y. Noh, M. Tang, and K. S. Liang, Appl. Phys. Lett. **81**, 5120 (2002).

[28] N. Gogneau, D. Jalabert, E. Monroy, E. Sarigiannadou, J.-L. Rouvière, T. Shibata, M. Tanaka, J. M. Gérard, and B. Daudin, J. Appl. Phys. **96**, 1104 (2004).

[29] G. Capellini, M. De Seta, L. Di Gaspare, F. Evangelisti, and F. d'Acapito, J. Appl. Phys. **98**, 124901 (2005).

[30] J. Brault, M. Gendry, O. Marty, M. Pitaval, J. Olivares, G. Grenet, and G. Hollinger, Appl. Surf. Sci. **162-163**, 584 (2000).

[31] C. Priester and G. Grenet, Phys. Rev. B **64**, 125312 (2001).